

Florida Institute of Technology

Scholarship Repository @ Florida Tech

Electrical Engineering and Computer Science
Faculty Publications

Department of Electrical Engineering and
Computer Science

7-2-1998

Wavelet-based noise reduction in multispectral imagery

Abdullah A. Basuhail

Samuel Peter Kozaitis

Follow this and additional works at: https://repository.fit.edu/ces_faculty



Part of the [Electrical and Computer Engineering Commons](#)

PROCEEDINGS OF SPIE

[SPIDigitalLibrary.org/conference-proceedings-of-spie](https://spiedigitallibrary.org/conference-proceedings-of-spie)

Wavelet-based noise reduction in multispectral imagery

Abdullah A. Basuhail
Samuel Peter Kozaitis

SPIE.

Wavelet-based noise reduction in multispectral imagery

Abdullah A. Basuhail, and Samuel P. Kozaitis
Florida Institute of Technology
Division of Electrical and Computer Science and Engineering
150 W. University Blvd.
Melbourne, FL 32901

ABSTRACT

We used a 3-D wavelet-based denoising method to reduce the noise from multispectral imagery. In our approach, we compared denoising of different bands of a multispectral image using a 2-D denoising technique, by which the wavelet coefficients corresponding to each band were denoised independent of each band, and a 3-D denoising technique by which the wavelet coefficients were denoised by involving all bands in thresholding the wavelet coefficients. Due to the high correlation of the multispectral imagery data along the wavelength axis, the noise can be easily reduced by applying the wavelet transform along the wavelength direction. Our results showed that the 3-D denoising approach improved the overall SNR of a noisy multispectral imagery over the 2-D denoising approach, due to the correlation between the different bands.

Keywords: denoising, three-dimensional wavelet transform, multispectral.

1. INTRODUCTION

In multispectral imagery, a scene is acquired simultaneously in several spectral bands using a particular sensor. A scene imaged in this manner produces n digital images, where n is the number of bands acquired. The bands can be visualized as a cube of 3-D data. Any point in this cube can be represented by the space coordinates (x, y, λ) , where x, y are the spatial coordinates of a pixel in a certain band, and λ represents the wavelength information for that pixel. Multispectral imagery may contain noise at some or all of the bands.

Recently, wavelet-based methods for noise reduction referred to as denoising have been introduced, and have showed success in removing noise from an image while preserving details.^{1,2} Generally, denoising is the process of taking the wavelet transform of an image, thresholding the wavelet coefficients, and then taking the inverse wavelet transform. Furthermore, there are several ways to choose and implement the threshold.^{3,4} Like the Fourier transform, the wavelet transform describes a function with basis functions. Unlike the Fourier transform the basis functions in the wavelet transform are localized in both the input and wavelet domain. This dual localization has some important consequences. One is that objects can often be represented quite sparsely in the wavelet domain. The denoising process works primarily because the wavelet transform compacts energy more efficiently than other transforms such as the Fourier transform.

Denoising has at least two important properties. In general, a denoised signal is as smooth as the original signal. This is important because the mean square error (MSE) measure alone does not indicate the presence of undesirable structures in a reconstructed signal. In addition, a denoised signal achieves almost the minimax mean square error over every one of a wide range of smoothness classes, including many classes where traditional linear estimators do not achieve the minimax rate.⁴

We used a three-dimensional denoising technique for the reduction of the noise from a multispectral imagery. For comparison purposes we used a two-dimensional denoising technique where each band was processed independent from the other bands.

In the next section we briefly described denoising. Then, we discuss the three-dimensional denoising as applied to our approach. We then describe the results of our approach, and we showed a comparison of our results to the other denoising method.

2. DENOISING

Denoising typically involves taking the wavelet transform of a signal, thresholding the wavelet coefficients, then taking the inverse wavelet transform. After calculating the wavelet transform of the scaled signal, the noisy wavelet transform coefficients are usually subjected to a soft or hard threshold. A hard threshold indicates that wavelet transform coefficients are retained only if their absolute value is greater than or equal to a threshold t , and is described as

$$\bar{W}f(a,b) = \begin{cases} Wf(a,b) & \text{if } |Wf(a,b)| \geq t \\ 0 & \text{if } |Wf(a,b)| < t, \end{cases} \quad (1)$$

where $Wf(a,b)$ are the wavelet transform coefficients of a signal $f(x)$, a is the scale, and b specifies translation. A soft threshold is similar to the hard threshold, but "pulls" the values of the wavelet transform toward zero rather than simply retaining them. The soft threshold is described as

$$\bar{W}f(a,b) = \begin{cases} \text{sgn}(Wf(a,b))(|Wf(a,b)| - t) & \text{if } |Wf(a,b)| \geq t \\ 0 & \text{if } |Wf(a,b)| < t, \end{cases} \quad (2)$$

where $\text{sgn}(x)$ is the sign of x .

The reconstruction of the thresholded data using the inverse wavelet transform has two properties. First, the output achieves almost the minimax MSE. Second, the output is as smooth as the input. Moreover, its complexity is only $O(n)$, and hence the approach is very efficient in practice.¹

There are several ways to choose a threshold for denoising.^{3,4} One threshold that is easy to implement, has been shown to work well for sparse data, and produces a good visual quality of a denoised signal is described as VisuShrink,¹

$$t = \sqrt{2 \log(M)} \cdot \sigma \quad (3)$$

where M is the number of wavelet coefficients to be thresholded, σ is the standard deviation of the noise. Since the noise is unknown, its standard deviation value can be estimated by the median value of the wavelet coefficients at the finest scale. In order to avoid removing some of the signal which might appear at this scale, the value of the σ can be chosen such that half of the noise can be removed. This is significant from knowing that half of the Gaussian noise exists within $\pm 0.6745 \sigma$. The value of the standard deviation σ , of the noise can be estimated as,

$$\sigma = \text{median}(|Wf(a,b)|) / 0.6745 \quad (4)$$

where $Wf(a,b)$ is the wavelet coefficients of the noisy signal at the finest scale.

After thresholding, the inverse wavelet transform is performed on the thresholded coefficients. This thresholding method removes essentially all of the empirical wavelet coefficients that could (statistically) be attributed solely to noise. Fig. 1, illustrates the idea of the denoising technique of a 1-D signal corrupted with noise.

The denoising technique can be extended further to two or three dimensions, so that it can be used to denoise a two-dimensional data, e.g. an image, or a three-dimensional data, e.g. a multispectral image. In the next section we

discussed the three-dimensional denoising technique which we used in this work to reduce the noise in the bands of a multispectral imagery.

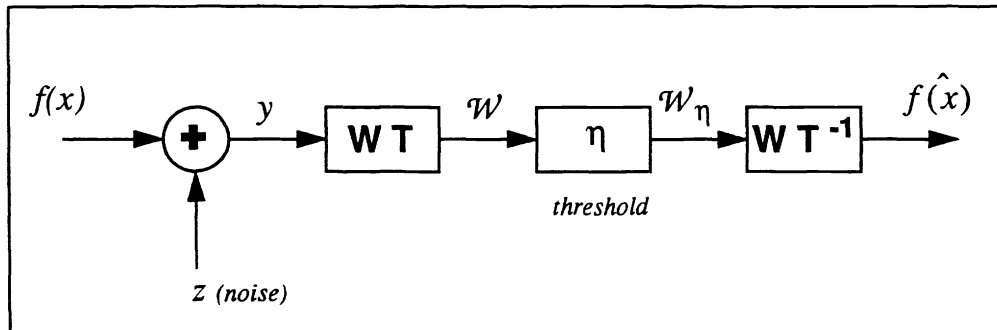


Figure 1. Signal denoising using the WT.

3. THREE-DIMENSIONAL DENOSING TECHNIQUE

As mentioned in the previous section, the denoising technique can be extended to three dimensions. A one dimensional wavelet transform structure can be used to transform a 3-D cube of data into the wavelet space. This is due to the fact that some wavelets are separable.

A 1-D wavelet transform can be applied to the entire data in the first dimension, which will result in spreading the input data into low- high-frequencies along the horizontal axis. In a similar manner, the 1-D wavelet transform will be applied to the resulted partially transformed data of the previous stage but in the second dimension. Finally, the transformed data resulted from the previous two steps will be further transformed using a 1-D wavelet transform, which will be applied in the third dimension. By completing these three 1-D wavelet transforms, the original data cube will be completely transformed to the wavelet space. Each component in the resulting cube is considered as a wavelet coefficient that represents the frequency distribution of the input data.

The resulting wavelet coefficients cube is composed of eight sub-cubes. Each one of the sub-cubes represents the low and the high frequency components in each of the processed dimensions. Fig. 2, shows the eight sub-cubes resulted from the 3-D wavelet transform, and Table 1 summarizes the frequency distribution represented by each sub-cube.

The threshold value can be calculated in a similar way to Eq. (3). The noise standard deviation can be estimated as described by Eq. (4), where in this case the wavelet coefficient which will be used in estimating the value of the standard deviation of the noise are the ones which are related to the cubes 1 to 7 in Fig. 2. The cube number 0 in this case corresponds to the low frequency components in the three directions resulted from the first scale wavelet decomposition, and so it will be excluded.

The threshold value calculated as in Eq. (3) will be determined and applied to the wavelet coefficient cube in order to filter the noise contribution in the wavelet space. Finally, a 3-D inverse wavelet transform will be applied to the thresholded wavelet coefficient cube to restore all the multispectral imagery bands with the noise reduced and improved SNR.

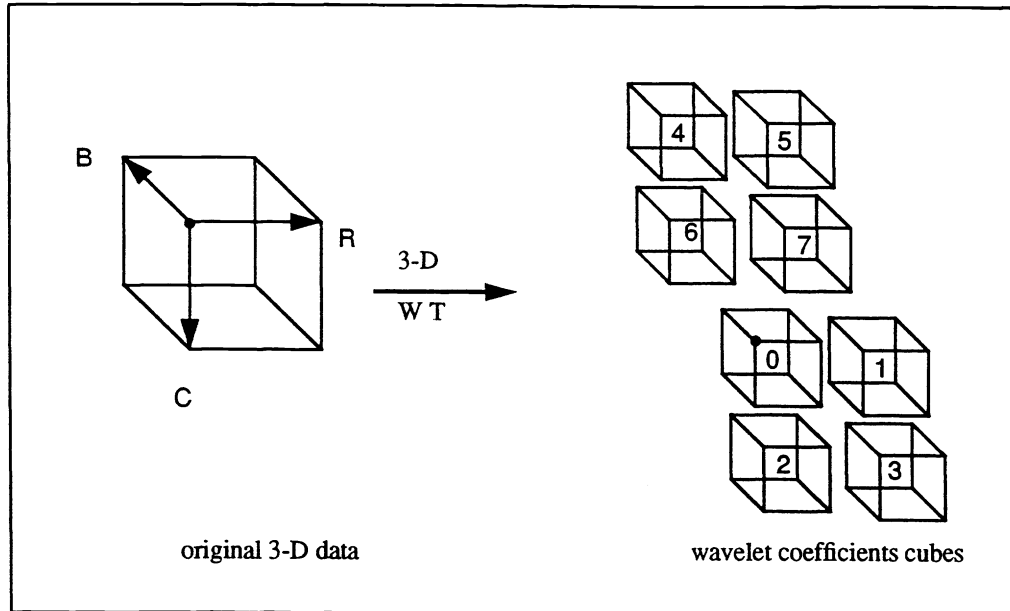


Figure 2. 3-D wavelet coefficients cubes.

Table 1: 3-D wavelet transform frequency distribution.

| Cube # | Band | Column | Row | Cube # | Band | Column | Row |
|--------|------|--------|-----|--------|------|--------|-----|
| 0 | L | L | L | 4 | H | L | L |
| 1 | L | L | H | 5 | H | L | H |
| 2 | L | H | L | 6 | H | H | L |
| 3 | L | H | H | 7 | H | H | H |

4. DENOISING OF MULTISPECTRAL IMAGERY

The denoising technique described in the previous section can be applied to a noisy multispectral imagery to reduce the effect of the noise from the different bands. We considered an n band multispectral image that contains zero-mean noise of unknown spectral density at each of the bands. Our goal is to maximize the energy compaction of the wavelet transform when using the correlation between the bands in a multispectral imagery. In the method, where the bands will be denoised independent of each other, the correlation information which occurs along the band direction will be lost, and consequently, the energy compaction will not be as efficient as in the 3-D case. This can be described as,

$$\sum W_f^2(a, b, \lambda) > \sum_{\lambda} \sum W_f^2(a, b) \quad (5)$$

5. RESULTS

We used an image in four different bands. Each band was corrupted with an independent gaussian noise distribution at 16 different SNRs. The bands were denoised using 2-D, and 3-D denoising techniques.

We compared both methods of denoising using the threshold in Eq. (3). In both methods we estimated the noise power (σ) by examining the wavelet transform of the multispectral imagery at the finest scale, and calculating the median of the wavelet coefficients for the two methods. We showed the results for one multi-band image shown in Fig. 3. The noisy image is shown as well as the denoised image for both methods using Daubechies 4-tap minimum phase wavelets.⁶

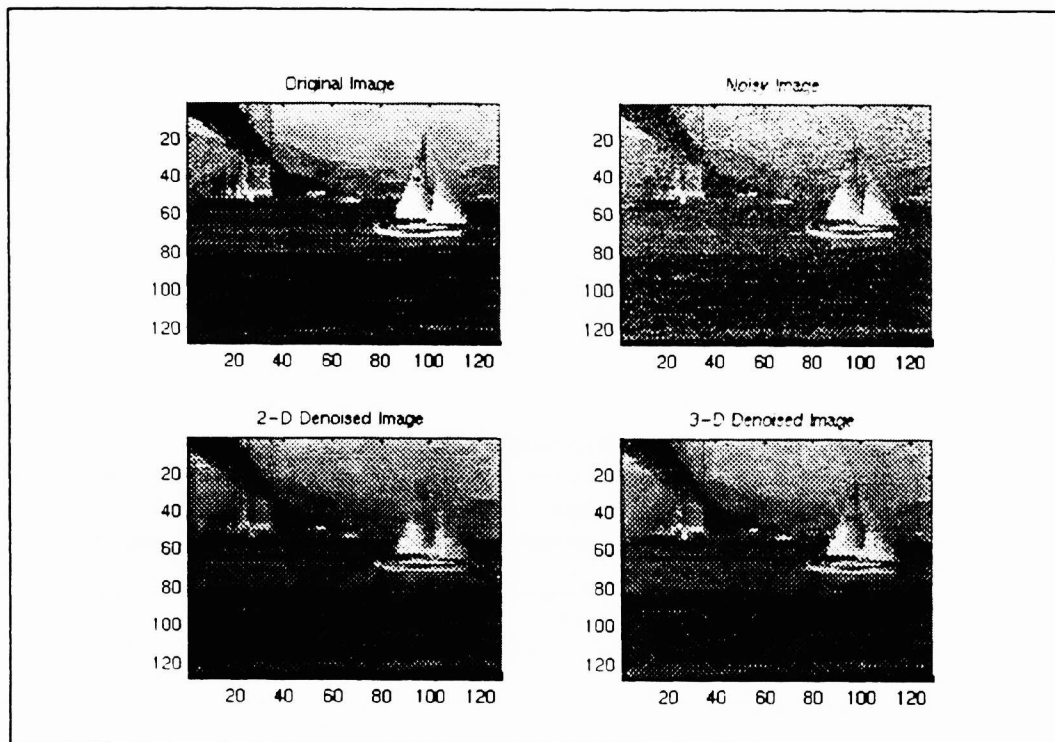


Figure 3. Multispectral image example.

Fig. 4, shows the relation between the energy of the thresholded wavelet coefficients and the SNR. As can be noticed from the graph, the total energy in the case of the 3-D approach is higher than the total energy of the 2-D approach. This means that the energy compaction is more efficient in the first case. From that plot, it can be concluded that, at SNR values less than 10, the energy compaction in the 2-D case starts to degrade, on the other hand, in the 3-D approach the energy compaction becomes more efficient.

The MSE and SNR values for the sum of the four bands using the two methods are indicated in Tables 1 and 2 and show superior results for the three dimensional denoising method.

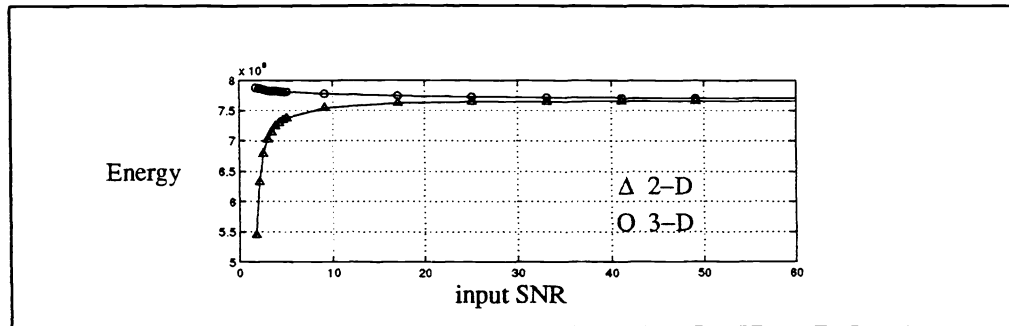


Figure 4. Energy of the thresholded wavelet coefficient at different input SNR.

Table 2: MSE using different noise removal approaches.

| # | original | 2-D | 3-D | # | original | 2-D | 3-D |
|---|----------|-------|-------|----|----------|--------|--------|
| 1 | 3133 | 2999 | 2263 | 9 | 58854 | 28801 | 19518 |
| 2 | 4618 | 3816 | 2848 | 10 | 67264 | 31753 | 21874 |
| 3 | 5885 | 4696 | 3386 | 11 | 78474 | 36099 | 25207 |
| 4 | 7848 | 5684 | 4080 | 12 | 94167 | 41808 | 29475 |
| 5 | 11771 | 7678 | 5506 | 13 | 117709 | 50922 | 35263 |
| 6 | 23543 | 13320 | 9155 | 14 | 156947 | 65669 | 44445 |
| 7 | 47084 | 23937 | 16307 | 15 | 235419 | 96734 | 62848 |
| 8 | 52314 | 26131 | 17710 | 16 | 470840 | 144383 | 118299 |

Table 3: SNR using different noise removal approaches.

| # | original | 2-D | 3-D | # | original | 2-D | 3-D |
|---|----------|-------|-------|----|----------|------|------|
| 1 | 59.90 | 62.60 | 82.90 | 9 | 3.20 | 6.50 | 9.60 |
| 2 | 40.60 | 49.20 | 65.90 | 10 | 2.80 | 5.90 | 8.60 |
| 3 | 31.90 | 40.00 | 55.40 | 11 | 2.40 | 5.20 | 7.40 |
| 4 | 23.90 | 33.00 | 46.00 | 12 | 2.00 | 4.50 | 6.40 |
| 5 | 15.90 | 24.40 | 34.10 | 13 | 1.60 | 3.70 | 5.30 |
| 6 | 8.00 | 14.10 | 20.50 | 14 | 1.20 | 2.90 | 4.20 |
| 7 | 4.00 | 7.80 | 11.50 | 15 | 0.80 | 1.90 | 3.00 |
| 8 | 3.60 | 7.20 | 10.60 | 16 | 0.40 | 1.30 | 1.60 |

Fig. 5, shows the relation between the MSE & SNR resulting from denoising the multispectral imagery and the input SNR. As can be concluded from the diagram the graphs the 3-D denoising method showed better results in terms of reducing the MSE and improving the overall SNR. From our experiments, we also found that in estimating the σ of the noise from the wavelet coefficients at the fine scale, when we used the cube which is representing the high frequencies in the three dimensions, namely cube number 7 (see Table 1), we were able to increase the overall SNR by about 2%. This is can be justified by the fact that this wavelet coefficient sub-cube contains almost all noisy coefficients, while on the other hand the six other sub-cubed are a mix of noise as well as some of the image data.

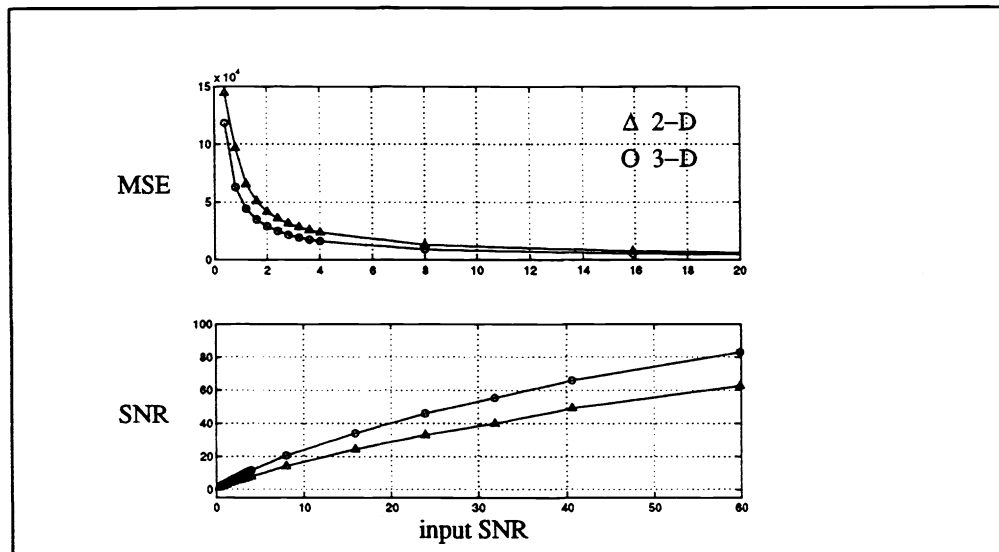


Figure 5. MSE & SNR at different input SNR noisy multispectral imagery.

6. CONCLUSION

We used a three-dimensional wavelet-based denoising method to reduce the noise from a multispectral image. In our approach, we applied a 3-D denoising technique for identification of wavelet coefficients not corrupted by noise. We found that denoising of multispectral imagery worked better when using a 3-D denoising technique was used compared to an independent 2-D denoising technique. In other words, the energy will be more compacted along the wavelength axis which will lead to an easier way to distinguish the noise contribution. We also found that using the wavelet coefficients representing the high frequencies in the three dimensions to estimate the σ of the noise improved the SNR value of the multispectral imagery.

7. REFERENCES

1. D. L. Donoho, "De-noising via soft thresholding," IEEE Trans. Inf. Theory, (May 1995).
2. D. L. Donoho, and I. M. Johnstone, "Ideal spatial adaptation via wavelet shrinkage," Biometrika, vol. 81,425-455 (1994).
3. D. L. Donoho, and I. M. Johnstone, "Ideal time-frequency denoising," Technical Report, Dept. of Statistics, Stanford University (1994).
4. D. L. Donoho, and I. M. Johnstone, G. Kerkyacharian, and D. Picard "Wavelet Shrinkage: Asymptopia," J. Roy. Statist. Soc. B 57 2 301-369 (1995).
5. T. P. Yu, A. Stoschek, and D. Donoho, " Translation- and direction- invariant denoising of 2-D and 3-D images: experience and algorithms." Proc. SPIE vol. 2825, 608-619, (1996).
6. I. Daubechies, "Orthonormal bases of compactly supported wavelets," Comm. Pure Appl. Math.,vol. 41,909-996 (1988).
7. T. Burns, S. Rogers, and M. Oxley, " Discrete, spatiotemporal, wavelet multiresolution analysis method for computing optical flow, " Optical Engineering, vol. 33, No. 7, 2236-2247, (1994).